

Reflectance measurements of human skin from the ultraviolet to the shortwave infrared (250 nm to 2500 nm)

Catherine C. Cooksey and David W. Allen
Sensor Science Division
National Institute of Standards and Technology
Gaithersburg, MD, USA 20899

ABSTRACT

While published literature of the optical properties of human skin is prevalent for the visible region, data are sparse in the ultraviolet and shortwave infrared. Spectral imaging has expanded from primarily an earth remote sensing tool to a range of applications including medicine and security applications, as examples. These emerging applications will likely benefit from exemplar data of human skin spectral signatures that can be used in designing and testing spectral imaging systems. This paper details an initial study of the reflectance properties over the spectral range of the ultraviolet to the shortwave infrared. A commercial spectrophotometer was used to collect the directional-hemispherical reflectance of each participant's skin from 250 nm to 2500 nm. The measurements are directly traceable to the national scales of reflectance and include estimated measurement uncertainties. The portion of skin under test was located on the participant's forearm and was approximately 5 mm in diameter. The results provided in this study serve as one point of reference for the optical properties of skin that in turn will aid in the development of physical and digital tissue phantoms.

Keywords: Skin, tissue, UV, light, SWIR, spectral, reflectance, traceable data, reference data

1. INTRODUCTION

Spectral imaging is rapidly finding its way into a wide range of applications. Some applications, such as those ranging from medical imaging to security and defense, will likely involve human subjects [1,2,3]. Much of the field of spectral imaging (from sensor design to processing algorithms) evolved around applications for earth remote sensing. One of the widely recognized limiting factors in spectrally based remote sensing is the lack of dependable spectral signatures for use as reference spectra. This issue has largely been addressed with libraries such as the Advanced Spaceborne Thermal Emission and Reflection Radiometer (ASTER) database, which provide spectra for a wide range of materials including minerals and vegetation [4]. While there is an abundance of data available on the optical properties of human skin, much of that information is focused on the visible part of the spectral region [approximately 400 nm to 700 nm] and the scattering properties (i.e. bidirectional reflectance distribution function or BRDF) over this region. The ultraviolet and shortwave infrared spectral regions generally have not been included in studies of the visible spectral region. This may have been due to less familiarity and, thus, less exploitation in combination with fewer sensing devices operating over those regions. Additionally, some of the data that are available do not provide sufficient details to understand the level of measurement uncertainty and the inherent variability within and between subjects.

One of the significant uses for the spectral signatures of human skin is its use as reliable reference data. In assessing the performance of spectral imaging sensor performance, optical standards are used. Ideally, the optical standard will represent the subject of interest by providing realistic spectral properties. Phantoms are often used as tissue proxies where either human subjects are either inconvenient, cannot be used, or consistency is important. The development of such phantoms requires a reliable model to base the design criteria. This includes both physical phantoms, such as those commonly used in the medical imaging community, and digital tissue phantoms, such as those produced by the NIST hyperspectral image projector (HIP) [5]

Property of the United States Government. Not subject to copyright. Correspondence: dwallen@nist.gov

In this study, we use a commercially available spectrophotometer with an integrating sphere accessory to measure the directional hemispherical reflectance of the forearm of human subjects. The forearm was selected as a sampling location because it is easily accessible, generally has less exposure to the sun, and also tends to have less hair relative to other areas. The intent is to collect a representative sample of skin reflectance spectra (a starting point for spectrally related research and development applications). We are not seeking to limit the measurement to a specific phenomenon (e.g., oximetric imaging). Rather, the goal is to express the measurement uncertainty and investigate/quantify the inherent biological variability of human skin (as an example, the sample position may include a vein in one scan and not the next due to a small displacement of the subjects arm).

2. METHOD

2.1 Human subjects

Twelve subjects volunteered to participate in this study.¹ They were solicited via advertisement. All of the subjects were federal employees. There was no attempt to select subjects based on age, gender, or ethnicity as might be related to skin tone. No subjects were excluded for the use of sun screen, body lotion, or medication, or for the presence of freckles, moles, tattoos, or skin conditions or disorders.

Prior to the beginning of the measurement session, each subject signed an informed consent form, which described the experiment and the benefits and risks of participation. Next, the researcher collected a photographic image of the test area on the subject's forearm. Finally, the reflectance measurements of the test area were acquired. Each subject participated in only one measurement session. Measurement sessions for the twelve subjects were scheduled over a period of several days.

2.2 Image collection

Image collection of the test area was intended to provide a means to document the uniformity of the general test region and to aid in the researchers' understanding of any significant variability that might be encountered. The researcher positioned the subject's bare right forearm behind a mask with a 5 cm aperture. A post, used as a hand grip, was positioned 25 cm from the center of the aperture. The camera, a Nikon D3000* digital single lens reflex (DSLR) camera with an 18 mm to 55 mm lens, was positioned 30 cm away. A ring illuminator was placed in front of the camera lens to provide near uniform illumination of the test area. Additionally, white and grey scale reference standards were placed around the aperture of the mask to ensure proper contrast adjustment of the image in post-processing. Several images were acquired for each subject.



Figure 1. The imaging setup showing the exposed sample area of the skin. The white and grey scale references surround the aperture of the mask. The camera is positioned to view through the ring illuminator.

¹ This human subject study, "Reflectance Measurements of Human Skin" Protocol #382, was approved by the NIST Institutional Review Board on May 29, 2012.

2.3 Reflectance measurement

The reflectance measurements of the volunteer's forearm were acquired using a commercial ultraviolet/visible/near-infrared spectrophotometer. An integrating sphere accessory was used with the spectrophotometer to acquire directional-hemispherical reflectance measurements. The integrating sphere has a diameter of 150 mm, an oval entrance port measuring approximately 15 mm by 25 mm, and a sample port diameter with nominal diameter of 25 mm. The sphere's coating is sintered polytetrafluoroethylene (PTFE). The sample beam of the spectrophotometer forms an image of the exit slit of the monochromator at the location of the sample port with an angle of incidence of 8° and dimensions of approximately 14 mm high by 6 mm wide. Because of the geometry of this measurement, the measurand is referred to as the $8^\circ/h$ spectral reflectance factor.

This approach is used in the same manner for the spectrophotometer measurement. This exposed area roughly matched the same sample area that was measured with the spectrophotometer.

The researcher positioned the subject's bare right forearm next to the sample port of the integrating sphere. Similar to the image collection setup, a post, used as a hand grip, was positioned 25 cm from the center of the sample port to ensure proper placement of the test area and consistency with the test area previously imaged. The subject was asked to maintain flush contact with the sample port without excessive pressure (as indicated by deep circular impressions of the sample port visible on the skin following the measurement). A swatch of black-light-proof fabric was laid over the arm and the room lights were dimmed to prevent ambient room light from contaminating the measurement. The spectrophotometer then acquired the reflectance measurement by scanning over the wavelength region of 250 nm to 2500 nm at a wavelength interval of 3 nm. A scan lasted approximately 3 minutes, and three scans were acquired for each subject. The subject was provided approximately three minutes to relax their arm between scans.

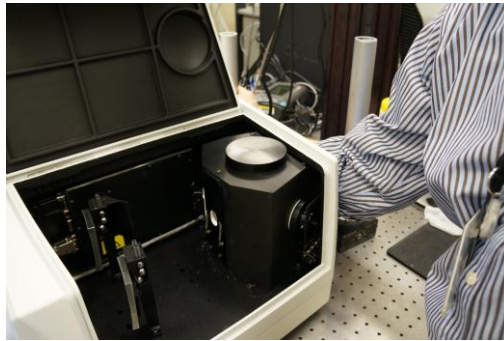


Figure 2. The spectrophotometer is shown with the cover in the open position to illustrate the location of the integrating sphere in relation to the arm.

The illuminating source was a deuterium lamp for wavelengths shorter than 319 nm and quartz-tungsten-halogen (QTH) incandescent lamp for longer wavelengths. The detector was a photomultiplier tube (PMT) for wavelengths shorter than 860 nm and a lead sulfide (PbS) or indium-gallium-arsenide (InGaAs) detector for longer wavelengths. For all measurements, the incident beam was depolarized using a 30 mm depolarizing element. The spectral bandwidth was fixed to 3 nm over the 250 nm to 860 nm spectral region; it was allowed to vary, with a maximum of 20 nm, over the 860 nm to 2500 nm spectral region.

The reflectance values acquired using this spectrophotometer were determined by relative measurement, requiring comparison to a reflectance standard. The standard was sintered PTFE. The reflectance scale for the reflectance standard was determined prior to the measurement sessions through comparison measurements of sintered PTFE and pressed PTFE. The scale for spectral reflectance factor was established for pressed PTFE in the NIST Spectral Tri-function Automated Reference Reflectometer (STARR) facility [6] using the absolute method of Van den Akker [7]. The wavelength scale of the spectrophotometer was validated using the spectrophotometer's internal atomic emission lamps.

2.4 Analysis

The 8°/h spectral reflectance factor R at each wavelength λ of the item was calculated from

$$R(\lambda) = \frac{S(\lambda) - S_d(\lambda)}{S_s(\lambda) - S_d(\lambda)} \cdot R_s(\lambda), \quad (1)$$

where S is the average signal from the scan of the item, S_s is the average signal from the scan of the standard, S_d is the dark signal, and R_s is the 8°/h spectral reflectance factor of the sintered PTFE standard. Dark signals were acquired once, prior to measurement sessions with subject. The final 8°/h spectral reflectance factors were obtained by averaging the values from the three scans.

An average spectrum of reflectance factors for the full set of scans acquired (36 scans) was calculated and compared to each spectrum in the set using the following equation, Equation 2, where S_1 is the mean of the full set of individuals and S_2 is each of the spectra for all individuals.

$$\theta = \cos^{-1} \left(\frac{S_1^T S_2}{\|S_1\| \|S_2\|} \right) \quad (2)$$

The difference between the spectra is reported in radians. The spectrum with the smallest resulting angle is considered to be the closest match to the average spectrum, and is selected as the representative of the mean. Selecting a representative spectrum from the overall set prevented the loss of spectral features that would have resulted from averaging the small shifts inherent in the spectral variability.

The estimated measurement uncertainties for the reflectance measurements are calculated according to the procedures outlined in [8]. Sources of uncertainty are the directional-hemispherical spectral reflectance factor of the sintered PTFE standard, the sphere geometry, the wavelength, and random effects. The uncertainty due to the standard was evaluated during the scale transfer from pressed PTFE, and determined to be 0.0045. The uncertainty due to the difference in sphere geometries of the commercial spectrophotometer used in the skin reflectance study and NIST STARR, which was used to establish the reflectance scale for the sintered PTFE standard, was evaluated by comparing reflectance factors of a NIST-owned sintered PTFE working standard measured using both instruments. The uncertainty caused by wavelength is evaluated from the derivative of the representative spectral reflectance factors of the mean. The repeatability was determined from the standard deviation of repeat measurements of the sintered PTFE standard. The expanded uncertainty ($k = 2$) is the combined (root-sum-square) uncertainty from all contributions due to systematic and random effects multiplied by a coverage factor of two [8]. The evaluated contributions of the sources of uncertainty and the expanded uncertainty ($k = 2$) of the instrument are given in Table 1. These uncertainties are representative of the manner in which the instrument was used for this study (henceforth referred to as the instrument uncertainty) and may not represent the best performance.

Table 1. Measurement uncertainties

Source of Uncertainty	Standard Uncertainty	Uncertainty Contribution
Reflectance Standard	0.0045	0.0045
Geometry	0.001	0.001
Wavelength	0.3 nm	0.0008
Repeatability	0.0003	0.0003
		Expanded Uncertainty ($k = 2$)
		0.0094

The variability observed for each subject due to the dynamic nature of human skin was calculated using the standard deviation of the three scans of each subject. The (population) variability observed for the set of subjects was calculated using the standard deviation of the full set of scans.

3. RESULTS

The results of the spectral reflectance measurements were examined at a general level without any specific application in mind. The images of the subject's test area are shown in Figure 3. Inspection of the images reveals that each subject's skin is generally uniform within the test area with only a minimal presence of veins and hair. The images of the test areas are provided for a qualitative analysis only.



Figure 3. Images of each subject's test area are shown for a qualitative assessment of the uniformity.

The reflectance spectrum shown in Figure 4 is the representative of the mean. This representative spectrum was selected using Equation 2. The best match between the mean and measurements was 0.017 radians while the largest difference was 0.24 radians. The noise level of the measurement is negligible and only becomes apparent at a low level near 2500 nm. There is a small effect from the detector crossover at 860 nm, resulting in a discontinuity. The effect of the detector crossover is also noted in the plot of the first derivative, shown below in Figure 7.

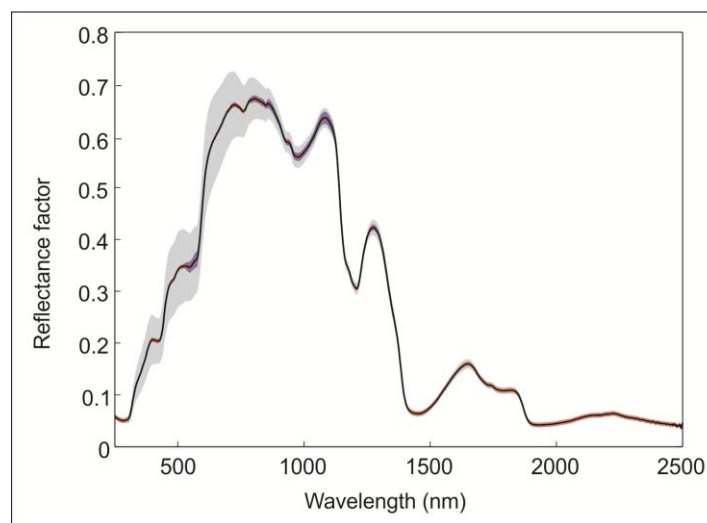


Figure 4. The reflectance spectrum of the representative of the mean with shaded areas representing the instrument uncertainty (red), subject variability (purple), and population variability for all subjects (grey).

The instrument uncertainty, subject variability (for the representative of the mean), and population variability are also depicted in Figure 4 to show their relative contributions as a function of wavelength. Throughout the ultraviolet (UV), visible (Vis), and near infrared (NIR) spectral regions, the population variability is the most significant source of uncertainty for the skin's spectral signature. Beyond 1100 nm, the contribution due to population variability decreases to a level on par with the instrument uncertainty. These contributions can be more clearly seen in Figure 5, which plots the instrument uncertainty, subject variability (for each subject with respect to their mean), and the population variability. There is an overall trend, as a function of wavelength, for the subject variability except for two subjects. The nature of these anomalous results is unknown. The population variability has a maximum at 620 nm and is as much as 3 times larger than the subject variability over the UV-Vis-NIR region. In the shortwave infrared (SWIR), the population variability is comparable to or less than that of the instrument uncertainty.

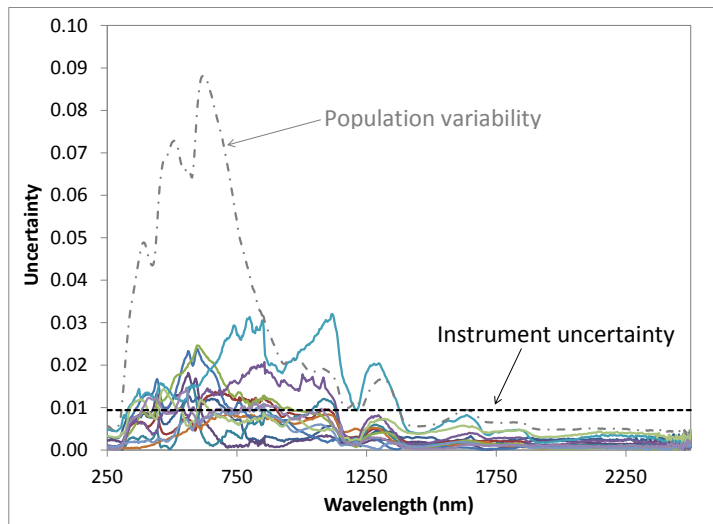


Figure 5. The instrument uncertainty (black dashed line), subject variability for each subject (solid colored lines) and population variability for all subjects (grey dot-dashed line).

The absorption spectrum is the net effect of the tissue constituents, including blood, water, and melanin, in addition to sweat glands, hair follicles, and collagen. The overall absorption spectrum is dominated by water, primarily at wavelengths shorter than 400 nm and longer than 1000 nm. The so called “therapeutic window” referred to with regard to medical imaging applications, extends from approximately 600 nm to 1300 nm [10]. This window coincides with the minima band in Figure 6. The spectral features commonly noted in the absorption spectra of whole blood, classic “W” feature near 600 nm, are largely smoothed by the contribution of the other constituents.

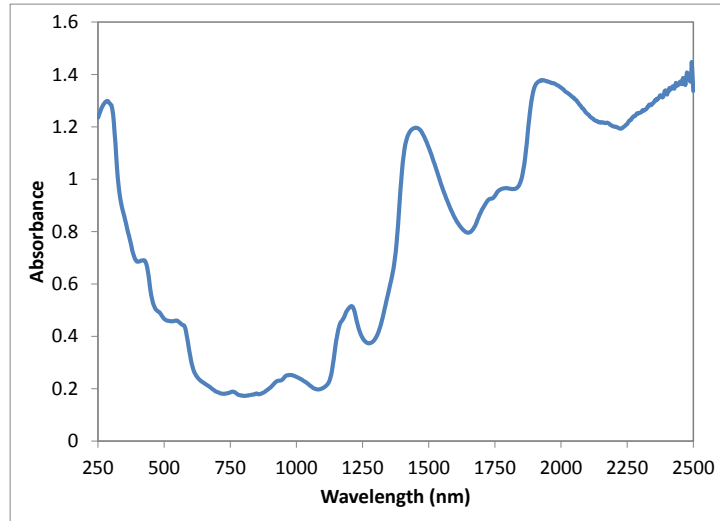


Figure 6. The representative mean absorption spectrum for the full spectral range.

The first derivative of each subject's mean reflectance spectrum is shown in Figure 7. This plot aids in defining the most significant absorption features. When comparing the full set of our subject's spectra, it is often difficult to distinguish the common spectral features among the varying levels of reflectance factor. The first derivative easily enables viewing of the peak locations, and provides a quantitative method for grouping spectra with similar spectral features. As noted in Figure 7, some of the features are not as easily identifiable for some subjects.

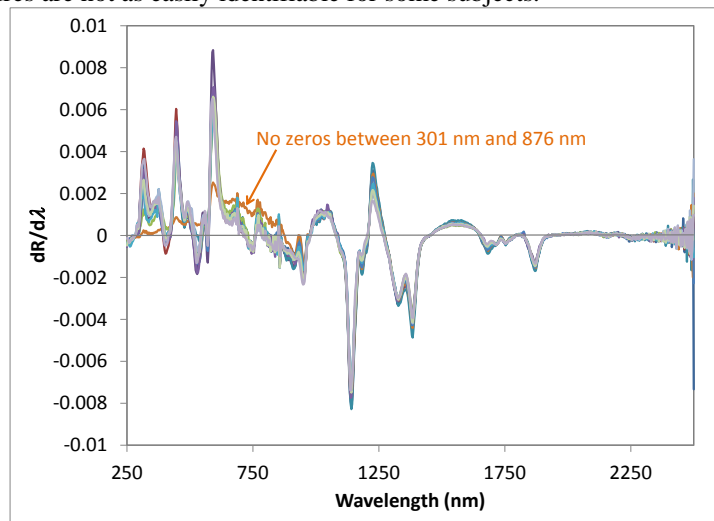


Figure 7. The first derivative of each subject's mean spectrum showing the reflectance features. Not all subjects displayed prominent spectral features in the visible and near-infrared regions.

4. DISCUSSION

The images provide a qualitative visual assessment of the degree of uniformity of the area of skin observed. Of this set of subjects, no significant features that might be expected to significantly affect the results were observed. The data presented in Figures 4 and 5 show that the instrument uncertainty can be significantly smaller than the standard deviation of the three scans of the same subject in the visible and near-infrared regions. There can be significant subject and

population variability in these spectral regions, which include regions often used to spectroscopically resolve tissue oxygenation, i.e. 500 nm to 1000 nm. In contrast, the short wave infrared was exceptionally consistent across all measurements (on the order of 1 %). The subject variability showed a similar pattern for most individuals; however there are two subjects that displayed significant differences that cannot be explained in this limited study. The first derivative spectra show many distinct features, typically attributed to the absorption due to oxy- and deoxyhemoglobin and water. These results also indicate that not all spectral features are resolvable, likely due to variable melanin content. For overall reflectance, the greatest differences between subjects at any one wavelength were below 10 %.

While this study does not adequately represent a sufficient proportion of the population, it does suggest that the instrument uncertainty is reasonably insignificant relative to the inherent variability between subjects. The variability for a given subject and the sample population, as a function of wavelength, is considerable. The spectral regions where there is significant variability may be useful in further exploiting these features. An expanded sample size would likely be useful in establishing the nature of these patterns.

The measurements presented here provide a small sample set of skin reflectance spectra over a broad spectral range. The results presented here may be used as one reference point for researchers who might need an example of a generalized skin reflectance spectrum. This data may be useful in research and development applications where there may have been insufficient or unreliable representations of human skin reflectance. This report is in no way intended to be a comprehensive study; instead it provides preliminary data and a cursory look at one possible method that may be repeated by other organizations. A significantly larger sample size will be needed to be more representative of the range of skin tones inherent in the general population.

5. SUMMARY

We have provided a sample set of reflectance spectra of human skin for use as reference data using a directional hemispherical geometry. The measurements are accompanied with the measurement uncertainties and the relative variability. The measurements are directly traceable to the national scale of reflectance. The measurement uncertainty is significantly smaller than the inherent variability of the skin reflectance. The spectral regions of inherent variability of the measurements due to biological factors are a topic of further exploration. This data will help in establishing the foundation for a model for both physical and digital tissue phantoms. Beyond the preliminary data presented, the method is also one simple approach that may be considered in future experiments.

ACKNOWLEDGEMENTS

The authors would like to thank Nicholas Paulter of the NIST Security Technologies Group for support and guidance on this research. We would also like to acknowledge the volunteers who took the time to contribute and were essential to this study.

*Note: References are made to certain commercially available products in this paper to adequately specify the experimental procedures involved. Such identification does not imply recommendation or endorsement by the National Institute of Standards and Technology, nor does it imply that these products are the best for the purpose specified.

REFERENCES

- [1] C. C. Cooksey, J. E. Neira, and D.W. Allen, "The evaluation of hyperspectral imaging for the detection of person-borne threat objects over the 400nm to 1700 nm spectral region," Proc. SPIE 8357, Detection and Sensing of Mines, Explosive Objects, and Obscured Targets XVII, 83570O (May 1, 2012); doi:10.1117/12.919432
- [2] C.C. Cooksey, D.W. Allen, "Investigation of the potential use of hyperspectral imaging for stand-off detection of person-borne IEDs," Proc. SPIE. 8017, Detection and Sensing of Mines, Explosive Objects, and Obscured Targets XVI 80171W (May 13, 2011) doi: 10.1117/12.883502

- [3] R. X. Xu, D.W. Allen, et al., Developing digital tissue phantoms for hyperspectral imaging of ischemic wounds, *Biomedical Optics Express*, Vol. 3, Issue 6, pp. 1433-1445 (2012), <http://dx.doi.org/10.1364/BOE.3.001433>
- [4] ASTER Spectral Library, <http://speclib.jpl.nasa.gov/> , last accessed 4/28/2013
- [5] J.P. Rice, et al. Hyperspectral image projector applications, *Proc. SPIE 8254, Emerging Digital Micromirror Device Based Systems and Applications IV*, 82540R (February 9, 2012); doi:10.1117/12.907898
- [6] P. Y. Barnes, E. A. Early, and A. C. Parr, "NIST Measurement Services: Spectral Reflectance," NIST Special Publication 250-48 (1998).
- [7] W. H. Venable, J. J. Hsia, and V. R. Weidner, "Establishing a Scale of Directional-Hemispherical Reflectance Factor I: The Van den Akker Method," *Journal of Research of the National Bureau of Standards*, 82, 29 (1977).
- [8] B. N. Taylor and C. E. Kuyatt, "Guidelines for Evaluating and Expressing the Uncertainty of NIST Measurement Results," NIST Technical Note 1297 (1994).
- [9] V. R. Weidner and J. J. Hsia, "Reflection Properties of Pressed Polytetrafluoroethylene Powder," *J. Opt. Soc. Am.* 71, 856 (1981).
- [10] T. Vo-Dinh, *Biomedical Photonics: Handbook*, CRC Press, 2003, Washington, D.C.